Through-Space and Through-Bond Mixed Charge Transfer Mechanisms on the Hydrazine Oxidation by Cobalt(II) Phthalocyanine in the Gas Phase

V. Paredes-García,*,† G. I. Cárdenas-Jirón,*,‡ D. Venegas-Yazigi,†,§ J. H. Zagal,|| M. Páez,|| and J. Costamagna||

Facultad de Ciencias Naturales, Matemáticas y del Medio Ambiente, Universidad Tecnológica Metropolitana, Av. José Pedro Alessandri 1242, Santiago, Centro para la Investigación Interdisciplinaria Avanzada en Ciencias de los Materiales (CIMAT), Universidad de Chile, Av. Blanco Encalada 2008, Santiago, and Departamento de Química de los Materiales and Laboratorio de Química Teórica, Departamento de Ciencias Químicas, Facultad de Química y Biología, Universidad de Santiago de Chile, Casilla 40, Correo 33, Santiago, Chile

Received: October 19, 2004; In Final Form: November 16, 2004

Two quantum chemistry theoretical models in the gas phase at the density functional theory B3LYP/LACVP(d) level of calculation are proposed to rationalize the hydrazine oxidation by cobalt(II) phthalocyanine (Co(II)Pc). This oxidation reaction involves the net transfer of four electrons. These theoretical models that are described in terms of energy profiles include a *through-space* mechanism for the transfer of the first electron of the hydrazine and a *through-bond* mechanism proposed for the transfer of the three electrons remaining. The main difference between both models arises from a one-electron and one-proton alternate transfer for model 1 and a two-electron and two-proton alternate transfer for model 2. The main problem for experimental studies is to determine if the first transfer corresponds to an electron or a chemical transfer. Under this point of view, we proposed two models which deal with this problem. We conclude that model 1 is more reasonable than model 2 because the whole oxidation process is always exergonic.

1. Introduction

Hydrazine (N_2H_4) is a very important organic compound because of its wide application in industrial, pharmaceutical, fuel cell, and biological fields due to its characteristic reactivity.[1] Thus, the oxidation of hydrazine to molecular nitrogen has been extensively studied over the past years,[2−5] and the mechanism and kinetics of hydrazine oxidation have been analyzed under a wide range of conditions, in solution and with several electrodes.[6] Because of the large overpotential of hydrazine at conventional electrodes, one promising approach to minimize overvoltage effects is through the use of an electrocatalytic process at chemically modified electrodes.[7] One important group of inorganic compounds utilized for electrode modification and used for electrocatalytic purposes is the metallo-phthalocyanines (MPc).[7,8] The catalytic activity of MPc is dependent on the central metal ion involved and on the total oxidation state of the complex.[5] In the metallo-phthalocyanine set, cobalt phthalocyanine (CoPc) and substituted CoPc are expected to play an important role because of their electrocatalytic capability toward a wide variety of redox systems.[7−9] CoPc has been widely used in the electrooxidation of hydrazine, and different models for the electron transfer involved in this reaction have been proposed.[2,5,6,10]

In past years, our interest has been centered on the theoretical study of the electronic structure of transition metal porphyrins and derivatives and azamacrocycles, either as isolated complexes[5a,11−17] or as inserted in an oxidation−reduction process.[5a,14,18−21]

Theoretical studies based on quantum chemistry for diferent electron transfers involved in redox processes such as the 2-mercaptoethanol (2-ME)[14,19] and hydrazine[20] oxidations have been previously reported on cobalt phthalocyanine systems. In the case of the 2-ME oxidation mediated by CoPc, we studied the effect of graphite (G) on the global reactivity.[19] To understand the effect of the graphite electrode on the reactivity of CoPc, we built interaction energy profiles along the reaction coordinate $r_{Co\cdots S}$ with and without the presence of graphite. We found that the presence of graphite leads to a process with the highest reactivity (lowest activation energy) in comparison to isolated CoPc. Numerical values of activation energies obtained from experimentally measured data for processes involving the electrochemical reactions between metallo-phthalocyanines adsorbed in a graphite electrode with 2-ME are in the range 1.8−3.7 eV.[22] Our theoretical value of activation energy for the G···CoPc···2-ME system of 3.4 eV is therefore a good result, because it is in the expected order.[19] The corresponding value of activation energy for the CoPc···2-ME system is 6.0 eV. Thus, the decrease in the activation energy due to the presence of graphite has a value of 2.6 eV. An important remark about this study is that the trend obtained in the interaction energy profile for both G···CoPc···2-ME and CoPc···2-ME systems is the same. Then, a quantum chemistry theoretical study of the interaction CoPc···2-ME can be carried out without the presence of graphite, thus avoiding the large size of the graphite-containing system, and reducing the computational time.

We have also studied this system (CoPc···2-ME) from the point of view of charge transfer (CT) reactivity descriptors.[14] In this theoretical study, the global and local charge transfer descriptors were applied to a redox reaction and to a formation reaction (i.e., the redox reaction between cobalt phthalocyanine and 2-mercaptoethanol and the coordination interaction between

* To whom correspondence should be addressed. E-mail: vpg@manquehue.net (V.P.-G.); gcardena@lauca.usach.cl (G.I.C.-J.).
† Universidad Tecnológica Metropolitana.
‡ Laboratorio de Química Teórica, Universidad de Santiago de Chile.
§ Universidad de Chile.
|| Departamento de Química de los Materiales, Universidad de Santiago de Chile.

10.1021/jp045223g CCC: $30.25
Published on Web 01/22/2005

cobalt phthalocyanine and pyridine, respectively). Global and local property profiles were built up along a reaction coordinate defined between the atoms directly involved in each reaction. Two regions along the reaction coordinate were found for the redox reaction rationalized in terms of different kind of interactions (i.e., the *net* CT and no-interaction regions). However, the formation reaction only shows one region along the reaction coordinate, the formation region. We also found that local properties such as spin density and atomic net charge are good charge transfer descriptors, because they clearly show the difference between a net CT, the net transfer of one electron, and a *partial* CT along the reaction coordinate.[14]

On the other hand, we have proposed a first theoretical model to explain the trend in reactivity of CoPc and substituted CoPc for the oxidation of hydrazine.[20] Our study suggests that the reaction occurs via a *through-bond charge transfer* (TBCT) pathway and not via a *through-space charge transfer* (TSCT) pathway as was shown in previous work for the oxidation of 2-ME by CoPc.[14] We proposed a first mechanism for the oxidation of the hydrazine based on a four-step energy profile which agrees with the mechanism proposed at an experimental level for the electro-oxidation of hydrazine mediated by CoPc confined on a graphite electrode.[20] We showed that the step in the energy profile that involves the formation of a hydrazine radical seems to be a good starting point for the study of the transfer of the first electron in the oxidation of hydrazine mediated by different substituted Co(II)Pc.

In this work, we propose two theoretical models in the gas phase at density functional theory (DFT) level of calculation B3LYP/LACVP(d) to rationalize the hydrazine oxidation by cobalt(II) phthalocyanine based on an energy profile framework. These theoretical models mainly include a mechanism starting from the interaction between Co(II)Pc and the hydrazine residue $[N_2H_3]^-$ and ending with the formation of molecular N_2; the latter corresponds to the final product released after the four-electron oxidation. It is important to note that the mechanisms proposed here constitute a first approximation making use of the quantum chemistry tools, which is not available in the literature, and obviously can be improved and complemented with new theoretical and experimental studies.

2. Computational Details

All calculations have been carried out using the *TITAN* package.[23] The studied systems were cobalt(II) phthalocyanine (Co(II)Pc) and the hydrazine residue ($[N_2H_3]^-$) (Figure 1), and the molecular geometries were fully optimized at a semiempirical Hartree−Fock PM3(tm) (tm = transition metal) level of theory. Using the PM3(tm) optimized geometries as an initial guess, we performed single-point calculations at a density functional level of theory. We considered the Becke's three-parameter hybrid exchange functional (which includes the exact Hartree−Fock, Slater, and Becke exchanges) and the LYP correlation functional named as B3LYP.[24] All DFT calculations were performed using the LACVP(d) basis set which includes an effective core potential (ECP) with d orbitals for the cobalt atom and a 6-31G(d) basis set for the lighter atoms such as carbon, nitrogen, and hydrogen. It has been shown previously that the use of ECP reduces the computational time, and so, this methodology is recommended for the theoretical description of transition metal atoms, because the latter have many core electrons. We propose two models for the hydrazine oxidation on the basis of the energy profiles of the different stages starting from the interaction Co(II)Pc···$N_2H_3^-$ and ending with N_2 release. In these profiles, we have only considered the minimal energy states. Atomic spin densities and atomic electronic population were analyzed under the natural atomic orbital approximation.[25]

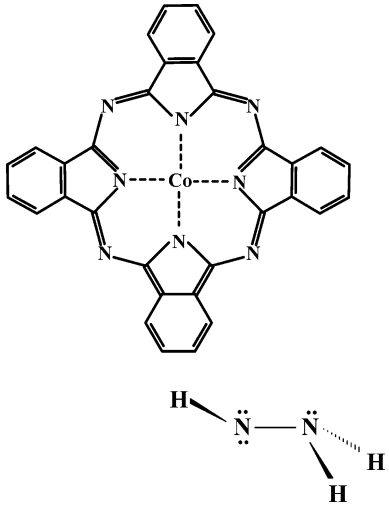

Figure 1. Molecular structure of cobalt(II) phthalocyanine (Co(II)Pc) and the anionic hydrazine ($[N_2H_3]^-$).

3. Results and Discussion

For the rationalization of the hydrazine (N_2H_4) oxidation by cobalt(II) phthalocyanine, we have studied the charge transfer mechanisms starting with the interaction between Co(II)Pc and the N_2H_4 neutral species. The study was done using a reaction coordinate corresponding to the distance between the cobalt atom and nitrogen of hydrazine of $r_{Co\cdots N} = 2.5$ and 4.0 Å. The results obtained indicated that no charge transfer occurred along the reaction coordinate. This suggests that the interaction between Co(II)Pc and N_2H_4 is not favored, and therefore, no redox process is observed. Some studies show that at experimental level the electro-oxidation of hydrazine occurs at strong basic pH (pH = 13).[4,6,7] Knowing that at pH = 4 99.9% of the hydrazine is present as the protonated species and at pH = 8 approximately 50% of the hydrazine is protonated and 50% is in neutral form,[4a] then, it is possible assume that at pH = 13 the protonated species is present in a much lower amount, and in consequence, the neutral species is the majority. On the basis of this fact, we suppose that with the existence of minimal quantities of anionic hydrazine ($N_2H_3^-$) at strongly basic conditions is enough for the catalytic processes. We will use the latter species to study the interaction with Co(II)Pc and investigate if $N_2H_3^-$ is a good form of hydrazine that allows us to visualize the oxidation process. This process ends with the formation of molecular N_2. The $[N_2H_3]^-$ species was considered on the basis of experimental studies[4b,6,7] where the electro-oxidation is carried out in a strong basic media. In aqueous solution, the following equilibrium for hydrazine is strongly favored for the formation of products: $N_2H_4 + OH^- \Leftrightarrow N_2H_3^- + H_2O$. Because the anionic hydrazine ($N_2H_3^-$) undergoes some changes during the oxidation process, we will name it as the hydrazine residue. In this section, we present two possible mechanisms obtained at a theoretical level using the quantum chemistry tools. These mechanisms will be named throughout the article as model 1, which is shown in Schemes1 and 2, and model 2 that is displayed in Schemes1 and 3. To perform the energy profile study of the whole oxidation process that will be discussed in section 3.4, we considered in both models a complete mass and charge equilibrium, which then implied consideration of each equilibrium species such as CoPc, $[CoPc]^-$, H_2O, and OH^-. Models 1 and 2 consider in a first

SCHEME 1: Schematic Reactions Description for the Model 1 and Model 2 Mechanism. Steps A and B.

$$N_2H_4 + 4OH^- \rightleftharpoons N_2H_3^- + H_2O + 3OH^-$$

$$5[Co(II)Pc] + N_2H_3^- + H_2O + 3OH^- \longrightarrow [Co(II)Pc\cdots N_2H_3]^- + 4[Co(II)Pc] + H_2O + 3OH^- \quad A$$

$$[Co(II)Pc{-}N_2H_3]^- + 4[Co(II)Pc] + H_2O + 3OH^- \longrightarrow [Co(II)Pc{-}N_2H_3] + 3[Co(II)Pc] + [Co(I)Pc]^- + H_2O + 3OH^- \quad B$$

SCHEME 2: Schematic Reactions Description for the Model 1 Mechanism. Steps C to J.

$$[Co(II)Pc{-}N_2H_3]^- + 4[Co(II)Pc] + H_2O + 3OH^- \longrightarrow [Co(II)Pc{-}N_2H_3] + 3[Co(II)Pc] + [Co(I)Pc]^- + H_2O + 3OH^- \quad C$$

$$\downarrow$$

$$[Co(II)Pc{-}N_2H_2]^- + 3[Co(II)Pc] + [Co(I)Pc]^- + 2H_2O + 2OH^- \quad D$$

$$\downarrow$$

$$[Co(II)Pc{-}N_2H_2] + 2[Co(II)Pc] + 2[Co(I)Pc]^- + 2H_2O + 2OH^- \quad E$$

$$\downarrow$$

$$[Co(II)Pc{-}N_2H]^- + 2[Co(II)Pc] + 2[Co(I)Pc]^- + 3H_2O + OH^- \quad F$$

$$\downarrow$$

$$[Co(II)Pc{-}N_2H] + [Co(II)Pc] + 3[Co(I)Pc]^- + 3H_2O + OH^- \quad G$$

$$\downarrow$$

$$[Co(II)Pc{-}N_2]^- + 4[Co(I)Pc]^- + 3H_2O + OH^- \quad H$$

$$\downarrow$$

$$[Co(II)Pc{-}N_2] + 4[Co(I)Pc]^- + 4H_2O \quad I$$

$$\downarrow$$

$$[Co(II)Pc] + 4[Co(I)Pc]^- + N_2 + 4H_2O \quad J$$

SCHEME 3: Schematic Reactions Description for the Model 2 Mechanism. Steps C to J.

$$[Co(II)Pc{-}N_2H_3]^- + 4[Co(II)Pc] + H_2O + 3OH^- \longrightarrow [Co(II)Pc{-}N_2H_3] + 3[Co(II)Pc] + [Co(I)Pc]^- + H_2O + 3OH^- \quad C$$

$$\downarrow$$

$$[Co(II)Pc{-}N_2H_3]^+ + 2[Co(II)Pc] + 2[Co(I)Pc]^- + H_2O + 3OH^- \quad D$$

$$\downarrow$$

$$[Co(II)Pc{-}N_2H_2] + 2[Co(II)Pc] + 2[Co(I)Pc]^- + 2H_2O + 2OH^- \quad E$$

$$\downarrow$$

$$[Co(II)Pc{-}N_2H]^- + 2[Co(II)Pc] + 2[Co(I)Pc]^- + 3H_2O + OH^- \quad F$$

$$\downarrow$$

$$[Co(II)Pc{-}N_2H] + [Co(II)Pc] + 3[Co(I)Pc]^- + 3H_2O + OH^- \quad G$$

$$\downarrow$$

$$[Co(II)Pc{-}N_2H]^+ + 4[Co(I)Pc]^- + 3H_2O + OH^- \quad H$$

$$\downarrow$$

$$[Co(II)Pc{-}N_2] + 4[Co(I)Pc]^- + 4H_2O \quad I$$

$$\downarrow$$

$$[Co(II)Pc] + 4[Co(I)Pc]^- + N_2 + 4H_2O \quad J$$

stage an electron transfer occurring under a TSCT mechanism between CoPc and $[N_2H_3]^-$. Model 1 considers in the whole reaction two main steps in an alternate way, one of them involving a chemical transfer that implies a loss of one hydrogen atom, as a proton, and the second one involving the loss of one electron outside the molecular system. Model 2 also considers two main steps, one of them implying two consecutive electron losses outside the molecular system (one by each step), and the second one implying two consecutive hydrogen atoms as a proton loss (one by each step), until the oxidation process is completed. To simulate the whole electrocatalytic process for the anionic hydrazine oxidation that occurs at experimental level, in which the hydrazine residue is oxidized four times consecutively by the Co(II)Pc modified electrode, we represent at a theoretical level the oxidations of all species by performing calculations with $(N - 1)$ electrons for the oxidized species (N is the total number of electrons in the system). In the following section, we will analyze each model in detail. We include in Figures 2−4 the spin density surfaces (ρ^s's) of all molecular systems involved in both models that present an open shell. Table 1 summarizes the results obtained for ρ^s, cobalt−nitrogen (r_{Co-N}), and nitrogen−nitrogen (r_{N-N}) distances for models 1 and 2. Table 1 also includes information about the multiplicity of each of the structures involved in both mechanisms. For clarity, we present the results in three fragments: cobalt (Co), macrocycle (Pc), and hydrazine residue. Table 2 shows for the

TABLE 1: Spin Densities (ρ_i^s) and Bond Lengths r_{Co-N} and r_{N-N} (Å) for Each System Involved in the Oxidation Mechanism of the Anionic Hydrazine

Model 1

		ρ_i^s			bond length	
system	Co $(2S+1)^a$	Co	macrocycle	hydrazine residue	r_{Co-N}	r_{N-N}
$[CoPc\cdots N_2H_3]^-$	d	0.011	0.005	0.985	3.100	1.321
$[CoPc-N_2H_3]^-$	d	0.015	0.984	0.001	1.856	1.436
$[CoPc-N_2H_3]$	s				1.855	1.433
$[CoPc-N_2H_2]^-$	t	0.735	0.915	0.350	1.852	1.310
$[CoPc-N_2H_2]$	d	0.698	0.087	0.215	1.853	1.312
$[CoPc-N_2H]^-$	d	0.035	0.873	0.093	1.834	1.236
$[CoPc-N_2H]$	s				1.826	1.213
$[CoPc-N_2]^-$	t	0.822	1.080	0.098	1.817	1.110
$[CoPc-N_2]$	d	0.847	0.080	0.073	1.936	1.109

Model 2

		ρ_i^s			bond length	
system	Co $(2S+1)$	Co	macrocycle	hydrazine residue	r_{Co-N}	r_{N-N}
$[CoPc\cdots N_2H_3]^-$	d	0.011	0.005	0.985	3.100	1.321
$[CoPc-N_2H_3]^-$	d	0.015	0.984	0.001	1.856	1.436
$[CoPc-N_2H_3]$	s				1.855	1.433
$[CoPc-N_2H_3]^+$	d	0.000	1.000	0.000	1.854	1.431
$[CoPc-N_2H_2]$	d	0.698	0.087	0.215	1.853	1.312
$[CoPc-N_2H]^-$	d	0.035	0.873	0.093	1.834	1.236
$[CoPc-N_2H]$	s				1.826	1.213
$[CoPc-N_2H]^+$	d	0.000	1.000	0.000	1.829	1.217
$[CoPc-N_2]$	d	0.847	0.080	0.073	1.936	1.109

[a] $(2S+1)$ = spin multiplicity.

TABLE 2: Variation of the Total Energy (ΔE) (kcal/mol) and Electronic Population ($\Delta\rho_i$) for Each Step Included in the Oxidation Mechanism of the Anionic Hydrazine[a]

Model 1

		$\Delta\rho_i$		
step	ΔE	Co	macrocycle	hydrazine residue
A	−72.174	0.327	0.663	−0.990
B	0.469	−0.242	0.074	0.168
C	−11.296	0.005	−0.970	−0.034
D	−80.725	0.008	0.993	−1.000
E	−4.708	−0.012	−0.870	−0.118
F	−86.770	0.102	0.808	−0.909
G	−44.091	−0.032	−0.917	−0.051
H	−130.341	−0.066	1.046	−0.980
I	−20.790	−0.029	−0.920	−0.050

Model 2

		$\Delta\rho_i$		
step	ΔE	Co	macrocycle	hydrazine residue
A	−72.174	0.327	0.663	−0.990
B	0.469	−0.242	0.074	0.168
C	−11.296	0.005	−0.970	−0.034
D	90.451	0.002	−0.959	−0.043
E	−175.884	−0.006	1.082	−1.076
F	−86.770	0.102	0.808	−0.909
G	−44.091	−0.032	−0.917	−0.051
H	93.245	−0.016	−0.993	0.009
I	−244.376	−0.079	1.118	−1.039

[a] i refers to the fragment (Co, macrocycle, hydrazine residue). $\Delta E = E$(products) − E(reactants), where E(products) and E(reactants) correspond to the sum of the total energy associated to all the species present for the products and the reactants of each step.

same fragments the total energy change given by $\Delta E = E$(products) − E(reactants) where E(products) and E(reactants) correspond to the sum of the total energy associated with all the species present for the products and reactants of each step that appears in Schemes 1, 2, and 3. Table 2 also includes the atomic (i) electronic population change between consecutive steps for both models given by $\Delta\rho_i = \rho_i$(products) − ρ_i(reactants). Note that ρ_i(products) and ρ_i(reactants) correspond to the electronic population only of the species directly involved in the oxidation of the hydrazine residue, which is the latter and CoPc.

3.1. Through-Space: Model 1 and Model 2. To rationalize the first electron transfer between Co(II)Pc and the anionic

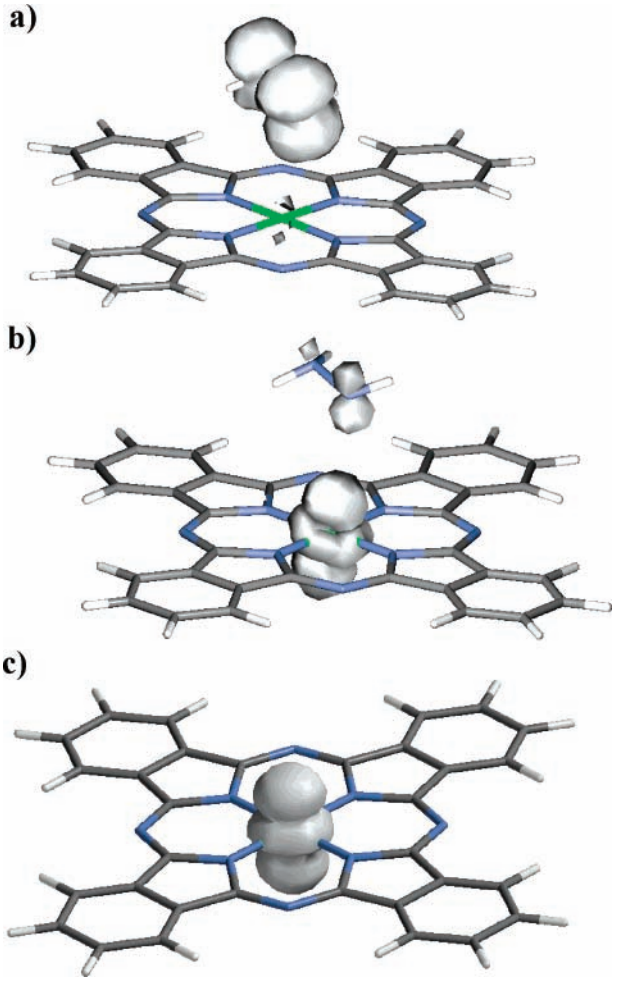

Figure 2. Spin-density surfaces calculated at B3LYP/LACVP(d) level of theory: (a) $[CoPc\cdots N_2H_3]^-$ at $r_{Co\cdots N} = 3.1$ Å distance; (b) $[CoPc\cdots N_2H_3]^-$ at $r_{Co\cdots N} = 3.2$ Å distance; (c) isolated Co(II)Pc.

species $[N_2H_3]^-$, we perform a full-geometry optimization of the system $[CoPc\cdots N_2H_3]^-$ along the reaction coordinate $r_{Co\cdots N}$, which is defined as the distance between the cobalt atom and one of the nitrogens of hydrazine. The study was performed between $r_{Co\cdots N} = 3.5$ and 3.0 Å, keeping fixed the distance between cobalt and nitrogen in each optimization. Then, the formation of the $[CoPc\cdots N_2H_3]^-$ species occurs through a van der Waals interaction, and we call it step A. We found that the

$$CoPc + N_2H_3{}^- \rightarrow [CoPc\cdots N_2H_3]^- \qquad \text{(step A)}$$

first electron transfer occurred at $r_{Co\cdots N} = 3.1$ Å. At this distance, the system presents a value of spin density of 0.985 on the hydrazine residue (see Table 1) and values near zero for the Co ($\rho^s = 0.011$) and macrocycle ($\rho^s = 0.005$) fragments, which indicates that the radical species is on the hydrazine fragment. These results indicate that the formation of a radical on the hydrazine residue due to the one-electron transfer from the latter to the CoPc fragment has occurred. Figure 2a shows the spin-density surface for $[CoPc\cdots N_2H_3]^-$ at distance $r_{Co\cdots N} = 3.1$ Å. To compare, we also include in Figure 2b the ρ^s surface at $r_{Co\cdots N} = 3.2$ Å. At this distance, we found that the CoPc and hydrazine residue do not present any interaction, and therefore, ρ^s is localized on the cobalt atom with a value of 0.8512. These results confirm at $r_{Co\cdots N} = 3.2$ Å the presence of Co(II) as it occurs in a Co(II)Pc isolated system (see Figure 2c). The transfer of the first electron from $[N_2H_3]^-$ to the CoPc fragment was also confirmed by the electronic population (see Table 2). In this table, we show that $\Delta\rho_i = -0.990$ for the hydrazine residue and has values of 0.327 and 0.663 for the cobalt and macrocycle fragments, respectively. These results indicate that the $[N_2H_3]^-$ fragment loses one electron, which is gained by the CoPc fragment. On the basis of our results, we propose that the first electron transfer from the $[N_2H_3]^-$ hydrazine residue to the Co(II)Pc fragment occurs by a through-space mechanism. Summarizing for models 1 and 2, the first electron transfer occurs via a TSCT mechanism leading to a radical hydrazine through a van der Waals interaction with the CoPc fragment.

3.2. Through-Bond: Model 1. For clarity, we will discuss separately in this section each step involved in model 1 displayed in Schemes 1 and 2, only considering the species that undergo a change. Once the first intermolecular charge transfer occurs between CoPc and $N_2H_3^-$, the $N_2H_3^\bullet$ radical species is coordinated to CoPc forming $[CoPc-N_2H_3]^-$, which is named as in step B. Note that the formation of this covalent species is

$$[CoPc\cdots N_2H_3]^- \rightarrow [CoPc-N_2H_3]^- \qquad \text{(step B)}$$

important, because it is the precursor species for the whole oxidation process. Therefore, we propose that the following stages of the oxidation process occur via a TBCT mechanism. $[CoPc-N_2H_3]^-$ presents an unpaired electron with a value of 0.984 for the spin density (Table 1, Figure 3a) localized on the macrocycle fragment instead on the hydrazine residue. In contrast to what was observed for $[CoPc\cdots N_2H_3]^-$, where a van der Waals interaction is present and a radical is localized on the hydrazine residue, the unpaired electron in $[CoPc-N_2H_3]^-$ is stabilized more effectively on the macrocycle when the interaction between CoPc and $[N_2H_3]^-$ is covalent. On the other hand, the results of $\Delta\rho_i$ obtained for step B (see Table 2) indicate that no net electron transfer occurs in the formation of $[CoPc-N_2H_3]^-$, but an intramolecular rearrangement in the entire system is observed. Then, the system is oxidized by one electron producing the $[CoPc-N_2H_3]$ neutral species

$$[CoPc-N_2H_3]^- \rightarrow [CoPc-N_2H_3] \qquad \text{(step C)}$$

The $[CoPc-N_2H_3]$ system can be a singlet (closed-shell system) or triplet (open-shell system) state. The singlet state gave a lower total energy value than the triplet state, and therefore, the closed-shell state was considered. Then, the $[CoPc-N_2H_3]$ species has a ρ^s value of 0.0. The variation of the electronic population ($\Delta\rho_i$) between the $[CoPc-N_2H_3]^-$ and $[CoPc-N_2H_3]$ species is presented in Table 2. We observed that the macrocycle fragment has a value of $\Delta\rho_i = -0.970$, indicating that this fragment presents a loss of one electron when the $[CoPc-N_2H_3]$ neutral species is formed.

In summary, the theoretical model predicts that the electron corresponding to the first oxidation of the hydrazine residue is released from the macrocycle fragment and not from the cobalt atom ($\Delta\rho_i = 0.005$), as would be expected.

To continue with the second-electron oxidation, it is necessary to lose a second hydrogen atom as a proton from the $[CoPc-N_2H_3]$ species, thus leading to an anionic species occurring by step D. The $[CoPc-N_2H_2]^-$ species could exist in a singlet or

$$[CoPc-N_2H_3] \rightarrow [CoPc-N_2H_2]^- \qquad \text{(step D)}$$

triplet state. In this case, we found that the total energy of the triplet state (open-shell system) was lower than the singlet-state value, and therefore, it was the most stable. Then, the $[CoPc-N_2H_2]^-$ species will present a value of $\rho^s = 2.0$. Table 2 shows

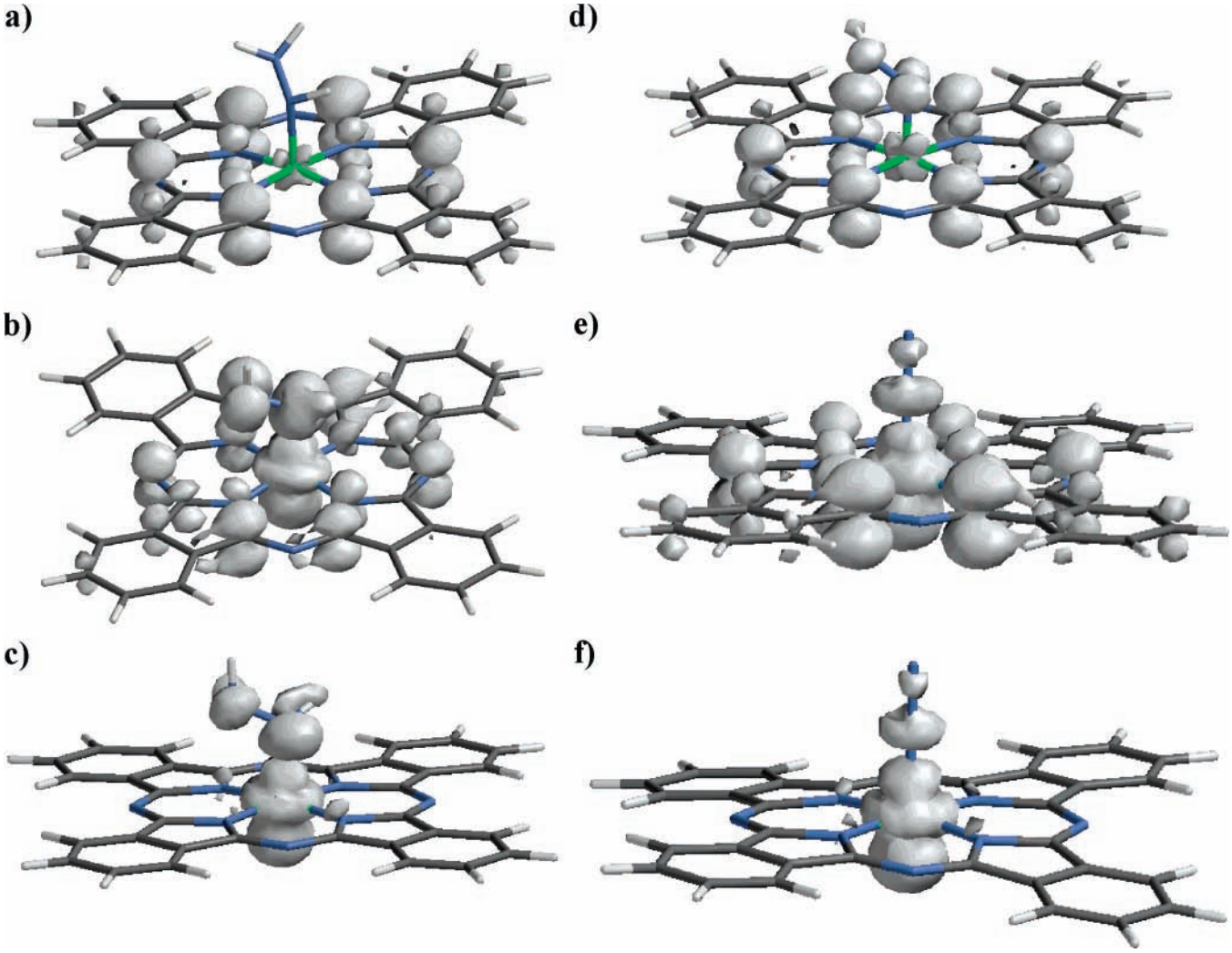

Figure 3. Spin-density surfaces calculated at B3LYP/LACVP(d) level of theory: (a) $[CoPc-N_2H_3]^-$, (b) $[CoPc-N_2H_2]^-$, (c) $[CoPc-N_2H_2]$, (d) $[CoPc-N_2H]^-$, (e) $[CoPc-N_2]^-$, (f) $[CoPc-N_2]$.

that $\Delta\rho_i$ associated with step D has values of -1.000 for the hydrazine residue and 0.993 for the macrocycle fragment. This suggests that, together with the loss of one hydrogen atom by the hydrazine residue in the $[CoPc-N_2H_3]$ species, one electron is transferred from the hydrazine to the macrocycle. Note that $\Delta\rho_i$ for cobalt is 0.008, meaning that this atom practically does not present any change in step D. The analysis of the electronic properties shows that the loss of a second hydrogen atom as a proton has involved an intramolecular charge transfer associated to one electron from the hydrazine residue to the CoPc system. The results showed for ρ^s in Table 1 indicate that the two electrons of the $[CoPc-N_2H_2]^-$ species corresponding to the triplet state are mainly localized on the macrocycle (0.915) and on the cobalt atom (0.735). A minor amount is localized on the hydrazine residue (0.350). This is a good result that, together with the results of $\Delta\rho_i$, anticipates that the one-electron oxidation from the $[CoPc-N_2H_2]^-$ species outside of the system would occur from the macrocycle. Figure 3b shows the surface of the spin density for $[CoPc-N_2H_2]^-$ and may show in a graphical way that ρ^s is mainly localized on the cobalt atom and on the macrocycle. This means that a cobalt(II) is present in this species. Once the $[CoPc-N_2H_2]^-$ species is produced, a second electron is removed from the system to continue the hydrazine residue oxidation process. Thus, we propose the following step

$$[CoPc-N_2H_2]^- \rightarrow [CoPc-N_2H_2] \qquad \text{(step E)}$$

The $[CoPc-N_2H_2]$ species is a doublet state that presents its frontier electron mainly on the cobalt atom, which can be viewed through the spin density showed in Table 1. The values obtained for ρ^s are 0.698 for the cobalt atom and 0.215 for the hydrazine residue. Figure 3c shows the surface of ρ^s obtained for this species. If we compare this figure with Figure 1, we can say that the cobalt atom in $[CoPc-N_2H_2]$ is nearly a cobalt(II). The results for $\Delta\rho_i$ associated to step E give a value of -1.094, indicating that a negative variation occurs on the macrocycle, which corresponds to the loss of one electron. The values of $\Delta\rho_i$ for the cobalt atom and the hydrazine residue are nearly zero. We can conclude that the removal of the second electron in the oxidation process of the hydrazine residue occurs by the macrocycle. To continue this oxidation process, we propose the removal of the third hydrogen atom as a proton from the $[CoPc-N_2H_2]$ species as identified by step F. The $[CoPc-N_2H]^-$ species

$$[CoPc-N_2H_2] \rightarrow [CoPc-N_2H]^- \qquad \text{(step F)}$$

is a doublet (open-shell system) state, and the spin-density value included in Table 1 shows that $\rho^s = 0.873$ for the macrocycle and presents values near zero for the cobalt atom and the hydrazine residue. Then, the frontier electron is mainly localized on the macrocycle. Figure 3d depicts the spin-density surface for $[CoPc-N_2H]^-$ obtained. On the other hand, $\Delta\rho_i$ shown in Table 2 indicates that the loss of one hydrogen atom as a proton

leads to an intramolecular charge transfer, with values of −0.909 for the hydrazine residue and 0.808 for the macrocycle. A small value of 0.102 for the cobalt atom was obtained. These results predict that the hydrazine residue lost nearly one electron, and the macrocycle gained nearly one electron, and so, we concluded that a charge transfer of nearly one electron occurred. The next step implies the outside removal of the third electron of the system, which we defined as step G. The $[CoPc-N_2H]$ species

$$[CoPc-N_2H]^- \rightarrow [CoPc-N_2H] \qquad \text{(step G)}$$

is a system than can have a singlet or triplet multiplicity. We found that the lower-energy system corresponds to the singlet state (closed-shell system) and therefore is the more stable state. Then, we considered the $[CoPc-N_2H]$ species as a singlet state. Because $[CoPc-N_2H]$ is a closed-shell system, $\rho^s = 0.0$. The results obtained for $\Delta\rho_i$ associated to step G give values of −0.917 for the macrocycle, −0.032 for the cobalt atom, and −0.051 for the hydrazine residue. This indicates that in all the fragments a loss of charge is observed, with the sum of them equal to one. However, the most important loss is observed in the macrocycle, which was also evident for the first and second removal of one electron. The loss of the fourth hydrogen atom as a proton gives rise to step H. The $[CoPc-N_2]^-$ species could

$$[CoPc-N_2H] \rightarrow [CoPc-N_2]^- \qquad \text{(step H)}$$

present a singlet or triplet multiplicity. We optimized this species with both multiplicities and obtained the triplet state as the minor energy, which therefore corresponds to the more stable state. Then, in the following, we only consider the triplet state for the $[CoPc-N_2]^-$ species, and therefore, the total value for $\rho^s = 2.0$. As may be seen in Table 1, the two electrons of the triplet state are mainly localized on the macrocycle ($\rho^s = 1.080$) and on the cobalt atom ($\rho^s = 0.822$), which is similar to the result obtained for the $[CoPc-N_2H_2]^-$ species. The spin-density surface for $[CoPc-N_2]^-$ is depicted in Figure 3e. The results of $\Delta\rho_i$ associated with step H, shown in Table 2, indicate that the macrocycle gained nearly one electron (1.046) and the hydrazine residue lost nearly one electron (−0.980). The cobalt atom does not present an important change in its electronic population ($\Delta\rho_i = -0.066$). In addition, we can see that the removal of the fourth hydrogen atom as a proton produces an intramolecular charge transfer from the hydrazine residue to the macrocycle, and the cobalt atom does not participate in the charge transfer. Finally, after the system has undergone the charge transfer, the loss of one electron from the system would occur, leading to step I. The formation of the $[CoPc-N_2]$ species

$$[CoPc-N_2]^- \rightarrow [CoPc-N_2] \qquad \text{(step I)}$$

anticipates that the oxidation process of the hydrazine residue is ending with the transfer of a fourth electron from the latter to the macrocycle. The $[CoPc-N_2]$ species is an open-shell system with a doublet multiplicity, and the value of ρ^s included in Table 1 indicates that the frontier electron is mainly localized on the cobalt atom ($\rho^s = 0.847$); see Figure 3f. The values of $\Delta\rho_i$ for step I show that the macrocycle has a value of −1.165; the other fragments present much reduced values. This means that the loss of the fourth electron from the system occurs again on the macrocycle, like what occurred with the previous outside oxidations. Finally, the last step that we define (step J) correspond only to the removal of molecular nitrogen (N_2) of the system.

$$[CoPc-N_2] \rightarrow CoPc + N_2 \qquad \text{(step J)}$$

Until this point, we may conclude that the oxidation process of a hydrazine residue may be modeled at a theoretical level using quantum chemistry based on a scheme that may be summarized as the following: (a) one hydrogen atom is removed as a proton (chemical transfer), and at the same time, an intramolecular transfer of one electron from the hydrazine residue to the macrocycle is occurring (intramolecular charge transfer); (b) one electron is removed outside of the system (outside charge transfer).

On the other hand, we also analyzed the structural changes of all the species studied in model 1. We found that, in the oxidation process of the hydrazine residue, the r_{Co-N} distances (see Table 1) decrease until the formation of $[CoPc-N_2]^-$, which could be favoring the charge transfer process. We also found that, in $[CoPc-N_2]$, the r_{Co-N} distance is larger than in the other species studied, with a value of 1.936 Å, indicating that the molecular nitrogen can be released. On the other hand, the r_{N-N} distances decrease in all the steps, which is in agreement with the formation of a triple bond in the molecular nitrogen. This distance is 1.109 Å, which is very close to the experimental distance value for molecular nitrogen (1.0897 Å).

3.3. Through-Bond: Model 2. In this model, steps B and C are the same as those discussed in section 3.2 for model 1 (Scheme 1). In contrast to that model, here step D corresponds to the loss of a second electron, following the equation

$$[CoPc-N_2H_3] \rightarrow [CoPc-N_2H_3]^+ \qquad \text{(step D)}$$

From Table 2, the value of $\Delta\rho_i$ for the macrocycle in step D is −0.959, indicating that this fragment lost one electron when the $[CoPc-N_2H_3]^+$ cationic species was formed. It is important to mention that the first and second electrons are lost from the macrocycle independent of the model used. We also found that the spin density in $[CoPc-N_2H_3]^+$ is localized only on the macrocycle (see Table 1, Figure 4a), meaning that the unpaired electron of the system is stabilized more effectively on this fragment. The next stage now involves the loss of a hydrogen atom as a proton

$$[CoPc-N_2H_3]^+ \rightarrow [CoPc-N_2H_2] \qquad \text{(step E)}$$

Through the values presented in Table 2 for $\Delta\rho_i$, it is possible to observe that, when the second proton is lost, the hydrazine residue loses one electron ($\Delta\rho_i = -1.076$), and the macrocycle fragment gains one electron ($\Delta\rho_i = 1.082$). This means that the loss of one hydrogen atom has always been associated with a through-bond charge transfer mechanism from the hydrazine residue to the CoPc fragment, also observed in model 1. The spin density for the cobalt atom in the $[CoPc-N_2H_2]$ species presents a value of 0.698 (Figure 3c), which nearly corresponds to a cobalt(II) atom. The third hydrogen atom loss, as a proton, is indicated by step F. As can be observed in Table 2, the

$$[CoPc-N_2H_2] \rightarrow [CoPc-N_2H]^- \qquad \text{(step F)}$$

hydrogen loss is again associated to a TBCT mechanism where the hydrazine residue loses nearly one electron ($\Delta\rho_i = -0.909$) and the CoPc fragment gains nearly one electron ($\Delta\rho_i = -0.910$). In the latter case, it is important to note that the gain of one electron mainly occurs in the macrocycle ($\Delta\rho_i = 0.808$), as was found for step E of model 2 and for steps D, F, and H of model 1. In contrast to step E, the spin density is mainly

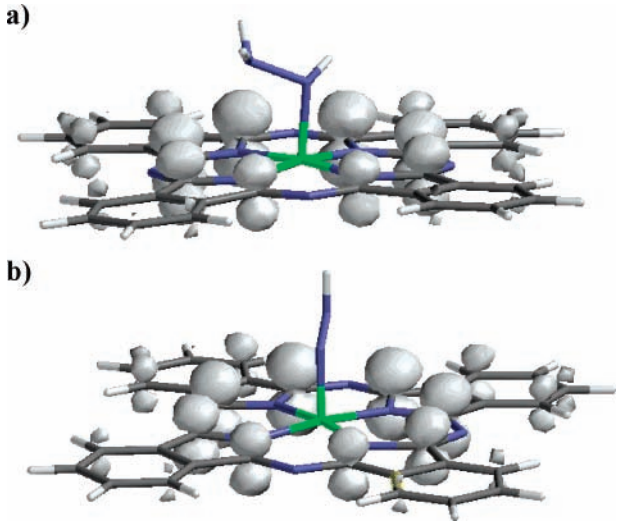

Figure 4. Spin-density surfaces calculated at B3LYP/LACVP(d) level of theory: (a) $[CoPc-N_2H_3]^+$, (b) $[CoPc-N_2H]^+$.

localized on the macrocycle fragment ($\rho^s = 0.873$, Figure 3d). The previous results can be understood as a system having the adequate electronic distribution for the next electron loss. The next stage corresponds to the third electron loss, depicted as step G. The $[CoPc-N_2H]$ species presents a singlet multiplicity;

$$[CoPc-N_2H]^- \rightarrow [CoPc-N_2H] \qquad \text{(step G)}$$

$\rho^s = 0.0$. The values obtained for $\Delta\rho_i$ for this species show again that the electron is lost from the macrocycle fragment ($\Delta\rho_i = -0.917$), as was seen in steps C and D of model 2 and in steps C, E, G, and I of model 1. The fourth electron loss is displayed in step H. $[CoPc-N_2H]^+$ presents a doublet multiplicity with a value of $\rho^s = 0.0$ for the cobalt atom and hydrazine residue and a value of $\rho^s = 1.0$ for the macrocycle fragment (Figure 4b), indicating that the unpaired electron is found on the macrocycle and not on the cobalt atom as would be expected. These results again confirm that the unpaired electron of the system is stabilized more effectively on the macrocycle fragment in CoPc. The $\Delta\rho_i$ values shown in Table 2 indicate that, as occurred in steps C, D, and G, the electron is removed from the system from the macrocycle fragment ($\Delta\rho_i = -0.993$). Finally, step I involves the loss of the last hydrogen atom as a proton. The spin-density values obtained for the $[CoPc-N_2]$ species show that the cobalt atom acquires the highest characteristic of cobalt(II) ($\rho^s = 0.847$, Figure 3f) like that observed for the $[CoPc\cdots N_2H_3]^-$ species at $r_{Co\cdots N} = 3.2$ Å (section 3.1). Note that $\rho^s = 0.956$ for the cobalt atom in an isolated CoPc system. The values of $\Delta\rho_i$ show that the hydrazine residue loses one electron ($\Delta\rho_i = -1.039$) and the macrocycle fragment gains one electron ($\Delta\rho_i = 1.118$). The last stage, corresponding to step J, involves the molecular nitrogen release, which was discussed in section 3.2.

$$[CoPc-N_2H]^+ \rightarrow [CoPc-N_2] \qquad \text{(step I)}$$

We can conclude the following for model 2: (a) the hydrogen atom removals from the system imply an intramolecular charge transfer defined by a through-bond charge transfer mechanism, (b) the electron removals from the system always occur from the macrocycle fragment.

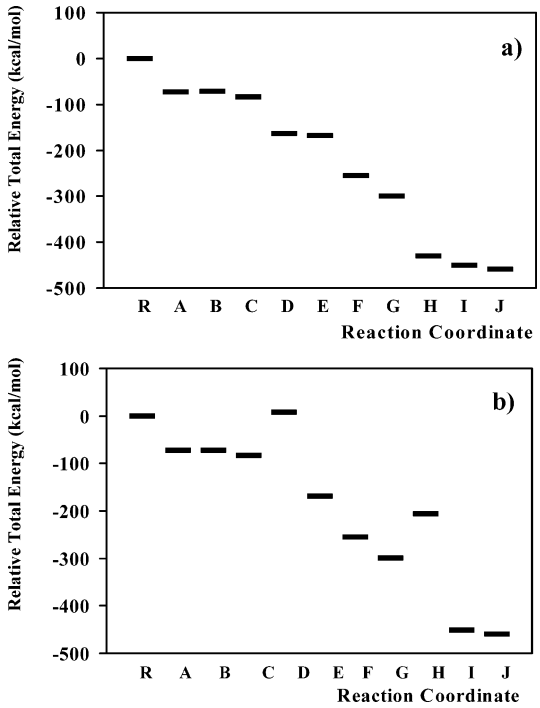

Figure 5. Potential energy profile calculated for the minimum-energy states at B3LYP/LACVP(d) level of theory: (a) model 1, (b) model 2. R = Reactants ([Co(II)Pc] and $N_2H_3^-$).

3.4. Energy Profile Analysis. To understand the oxidation of the anionic hydrazine to molecular nitrogen, which involves a four-electron transfer process, we built up a potential energy profile obtained only from minimum energy states. This is because we had some difficulties obtaining the corresponding transition states. In Figure 5a,b are presented the energy profiles for the whole redox process for models 1 and 2, respectively. In Figure 5a, it is possible to observe that the first electron transfer, occurring via a through-space charge transfer mechanism between Co(II)Pc and the anionic species $[N_2H_3]^-$ to form $[Co(II)Pc\cdots N_2H_3^-]$, is stabilized in ~72 kcal/mol. No significant change in the energy value (~0.5 kcal/mol) is observed when the covalent bonding between this species is formed (step B). The release of the first electron from the system, which is transferred from the hydrazine residue to Co(II)Pc described in step A, causes an energy stabilization of ~11 kcal/mol. A great energy stabilization of ~81 kcal/mol was calculated for the chemical transfer in step D (i.e., when a hydrogen ion is released at the medium). The second electron transfer out of the system causes an energy stabilization of only ~5 kcal/mol (step E). When the third hydrogen ion from the hydrazine residue is lost, the system is stabilized in ~87 kcal/mol (step F). The third electron transfer out the system described in step G stabilizes the system in ~44 kcal/mol. The last hydrogen ion is lost to generate the species shown in step H. This process causes a great energy stabilization of ~130 kcal/mol, suggesting that $[Co(II)Pc-N_2]^-$ species are more stable than $[Co(II)Pc-N_2H]$ species. Finally, the fourth oxidation, which leads to the full hydrazine oxidation process, stabilizes the system in ~21 kcal/mol (step I). In step J, molecular nitrogen is released and [Co(II)Pc] is reconstituted, and the system is stabilized only in ~9 kcal/mol. In the whole oxidation process, it is possible to observe from the first oxidation process until the last oxidation process a potential energy surface in the form of a cascade. This means that, for each chemical or electronic transfer, the system is always stabilized. The total energy difference from steps A to J (i.e., from the original reactants (Co(II)Pc interacting with the

$N_2H_3^-$ species) to the final products ([Co(II)Pc] and N_2)) is 459.3 kcal/mol.

For model 2, steps A, B, and C have the same energy change as the corresponding steps in model 1, as was mentioned in section 3.3. The second oxidation of the hydrazine residue described by step D destabilizes the system in ~90 kcal/mol. This destabilization may be associated with the formation of a cationic species. Later, two chemical transfers, which imply two hydrogen ions lost, are described by two consecutive steps (E and F). The system is stabilized in ~176 kcal/mol in step E and in ~87 kcal/mol in step F, indicating that in both steps the system releases energy, leading to a more stable state. Steps G and H describe the release of two electrons out of the system. The third electron released in step G stabilizes the system in ~44 kcal/mol; nevertheless, the fourth electron released in step H destabilizes the system in ~93 kcal/mol, like in step D. This again suggests that the formation of a cationic species promotes destabilization of the system. The next step produces the last chemical change, that is, the hydrogen ion is lost (step I), This change produces a stabilization of the system in ~244 kcal/mol. This value corresponds to the greatest energy change found for any step in both models. In step J, [Co(II)Pc] is reconstituted, and the nitrogen is released, as occurred in model 1. In this model, although the whole system presents a trend of diminishing energy values associated with each step, the cationic species formation produces an important destabilization. As in model 1, the energy difference between the original reactants (Co(II)Pc interacting with $N_2H_3^-$) and the final products ([Co(II)Pc] and N_2) is also 459.3 kcal/mol, but in model 2, the whole profile cannot be classified as a potential energy profile in the form of a cascade. Finally, it is important to note that at the experimental level the heat of combustion for hydrazine (N_2H_4), obtaining as the products molecular nitrogen and water, has a value of 149 kcal/mol.[26] Although this value is very different from that obtained in this work, it can be explained in terms of the different conditions under which both reactions occur.

4. Conclusions

In this work, we proposed two theoretical models to rationalize the hydrazine oxidation mediated by [Co(II)Pc]. For both models, we built energy profiles, and we found that the first three stages are the same for both models, and the most remarkable feature of these stages is that the first electron transfer occurs via a through-space charge transfer (TSCT) mechanism at a distance $r_{Co-N} = 3.1$ Å, leading to a hydrazine radical through a van der Waals interaction with the CoPc fragment.

The main difference between both proposals is that, in model 1, after a covalent bond is formed between [Co(II)Pc] and $N_2H_3^-$ (step C), electronic and chemical transfer occur in an alternate way. For model 2, two consecutive electrons are lost, and two chemical transfers occur. In model 1, only neutral and anionic species are produced, which is in agreement with the experimental conditions; however, for model 2, the formation of cationic species are proposed as intermediate stages, which correspond to destabilized forms in respect to the neutral and anionic forms. On the other hand in both models, every time than one hydrogen atom is removed as a proton (chemical transfer), an intramolecular transfer of one electron from the hydrazine residue to the macrocycle happens (intramolecular charge transfer). Therefore, the electron release from the molecular system (oxidation system process) always occurs from the macrocycle fragment (outside charge transfer). This fact is in agreement with experimental results, which suggests that the rate-limiting step is the first electron oxidation.

Also, it is possible to conclude that the outside charge transfer produces a lower stabilization than an intramolecular charge transfer, which is produced after the chemical transfer. In particular, model 1 always shows exergonic processes along the whole mechanism, while model 2 presents only two endergonic processes with the remaining corresponding to exergonic processes.

Acknowledgment. This work was supported by Project FONDECYT Lineas Complementarias no. 8010006/CHILE.

References and Notes

(1) (a) Li, X.; Zhang, S.; Sun, Ch. *J. Electroanal. Chem*. **2003**, *553*, 139. (b) Guerra, S. V.; Kubota, L. T.; Xavier, C. R.; Nakagaki, S. *Anal. Sci.* **1999**, *15*, 1231.

(2) Antoniadau, S.; Jannakoudakis, A. D.; Theodoridou, E. *Synth. Met.* **1989**, *30*, 295.

(3) Jiang, J.; Bian, Y.; Furuya, F.; Liu, W.; Choi, M.; Kobayashi, M.; Li, H. W.; Yang, Q.; Mak, T.; Ng, D. K. P. *Chem.—Eur. J*. **2001**, *7*, 5059.

(4) (a) Moliner, A. M.; Street, J. J. *J. Environ. Qual.* **1989**, *18*, 487. (b) Linares, C.; Geraldo, D.; Páez, M.; Zagal, J. H. *J. Solid State Electrochem*. **2003**, *7*, 626.

(5) (a) Cárdenas-Jirón, G. I.; Zagal, J. H. *J. Electroanal. Chem*. **2001**, *497*, 55. (b) Isaacs, M.; Aguirre, M. J.; Toro-Labbé, A.; Costamagna, J.; Páez, M.; Zagal, J. H. *Electrochim. Acta* **1998**, *43*, 1821.

(6) (a) Golabi, S. M.; Zare, H. R. *J. Electroanal. Chem.* **1999**, *465*, 168. (b) Trollund, E.; Ardiles, P.; Aguirre, M. J.; Biaggio, S. R.; Rocha-Filho, R. C. *Polyhedron* **2000**, *19*, 2303.

(7) (a) Razmi-Nerbin, H.; Pournaghi, M. H. *J. Solid State Electrochem.* **2002**, *6*, 126. (b) Zagal, J. H.; Lira, S.; Ureta-Zañartu, S. *J. Electroanal. Chem*. **1986**, *210*, 95. (c) Korfhage, K. M.; Ravichadran, K.; Baldwin, R. P. *Anal. Chem*. **1984**, *56*, 1514. (d) Pérez, E. F.; Neto, G.; Tanaka, A. A.; Kubota, L. T. *Electroanalysis* **1998**, *10*, 111.

(8) Halbert, M. K.; Baldwin, R. P. *Anal. Chem.* **1985**, *57*, 591.

(9) Wang, J.; Golden, T.; Li, R. *Anal. Chem*. **1988**, *60*, 1642.

(10) Golabi, S.; Noor-Mohammadi, F. *J. Solid State Electrochem*. **1998**, *2*, 30.

(11) Ríos-Escudero, A.; Costamagna, J.; Cárdenas-Jirón, G. I. *J. Phys. Chem. A* **2004**, *108*, 7253.

(12) Cárdenas-Jirón, G. I. *Int. J. Quantum Chem*. **2003**, *91*, 389.

(13) Cárdenas-Jirón, G. I.; Parra-Villalobos, E. *J. Phys. Chem. A* **2003**, *107*, 11483.

(14) Cárdenas-Jirón, G. I.; Venegas-Yazigi, D. A. *J. Phys. Chem. A* **2002**, *106*, 11938.

(15) Cárdenas-Jirón, G. I. *J. Phys. Chem. A* **2002**, *106*, 3202.

(16) Rios-Escudero, A.; Estiú, G.; Costamagna, J.; Cárdenas-Jirón, G. I. *J. Coord. Chem*. **2003**, *56*, 1257.

(17) Caro, C. A.; Bedioui, F.; Páez, M. A.; Cárdenas-Jirón, G. I.; Zagal, J. H. *J. Electrochem. Soc*. **2004**, *151*, E32.

(18) (a) Zagal, J. H.; Gulppi, M.; Isaacs, M.; Cárdenas-Jirón, G. I.; Aguirre, M. J. *Electrochim. Acta* **1998**, *44*, 1349. (b) Zagal, J. H.; Cárdenas-Jirón, G. I. *J. Electroanal. Chem*. **2000**, *489*, 96. (c) Cárdenas-Jirón, G. I.; Gulppi, M. A.; Caro, C. A.; del Río, R.; Páez, M.; Zagal, J. H. *Electrochim. Acta* **2001**, *46*, 3227.

(19) Cárdenas-Jirón, G. I.; Caro, C. A.; Venegas-Yazigi, D.; Zagal, J. H. *THEOCHEM* **2002**, *580*, 193.

(20) Venegas-Yazigi, D. A.; Cárdenas-Jirón, G. I.; Zagal, J. H. *J. Coord. Chem*. **2003**, *56*, 1269.

(21) Cárdenas-Jirón, G. I., Caro, C. A.; Zagal, J. H.; Páez, M.; Costamagna, J. In preparation.

(22) Caro, C. Lic. Sc. Thesis, Universidad de Santiago de Chile, Chile, 1999.

(23) *TITAN*, version 1.0.8; Wavefunction, Inc. and Schrodinger Inc., 18401 Von Karman Avenue, Suite 370, Irvine, CA 92612, U.S.A.

(24) (a) Lee, C.; Yang, W.; Parr, R. G. *Phys. Rev.* **1988**, *B37*, 785. (b) Miehlich, B.; Savin, A.; Stoll, H.; Preuss, H. *Chem. Phys. Lett.* **1989**, *157*, 200. (c) Becke, A. D. *J. Chem. Phys.* **1993**, *98*, 5648.

(25) (a) Weinhold, F.; Landis, C. R. *Chem. Ed.: Res. Pract. Eur*. **2001**, *2*, 91. (b) Weinhold, F. *J. Chem. Educ*. **1999**, *76*, 1141. (c) Foster, J. P.; Weinhold, F. *J. Am. Chem. Soc*. **1980**, *102*, 7211. (d) Reed, A. E.; Curtiss, L. A.; Weinhold, F. *Chem. Rev*. **1988**, *88*, 899. (e) Reed, A. E.; Weinhold, F. *J. Chem. Phys.* **1983**, *78*, 4066. (f) Reed, A. E.; Weinstock, R. B.; Weinhold, F. *J. Chem. Phys*. **1985**, *83*, 735.

(26) Petrucci, R.; Harwood, W. *General Chemistry: Principles and Modern Applications*; Prentice Hall International: Upper Saddle River, NJ, 1997.